Publishing House
AKAPIT

COMPUTER METHODS IN MATERIALS SCIENCE

Informatyka w Technologii Materiałów

Vol. 13, 2013, No. 1

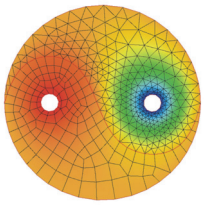

PREDICTION OF RESIDUAL STRESSES BY FE SIMULATIONS ON BIMETALLIC WORK ROLLS DURING COOLING

INGRID NEIRA TORRES[1,2,*], GAËTON GILLES[1], JÉROME TCHOUFANG TCHUINDJANG[3], JACQUELINE LECOMTE-BECKERS[3], MARIO SINNAEVE[4], ANNE MARIE HABRAKEN[1]

[1] Department ArGEnCo, Division MS2F, Université de Liège,
[2] Department of Materials Engineering, Universidad de Concepción,
[3] Departement M&S, Division LTAS MMS, Université de Liège,
[4] Marichal Ketin, Verte Voie 39B- 4000 Liège
**Corresponding author: ineira@doct.ulg.ac.be*

Abstract

Bimetallic rolls used in the roughing stands of the Hot Strip Mill require mixed properties as a high wear resistance for the shell material and an enhanced toughness for the core material. The bimetallic roll studied in this paper is obtained from a vertical spin casting process followed by cooling and subsequent heat treatments. Failure of the compound roll sometimes occurs during the cooling stage of the casting route or later during the thermal treatments. It requires to deeply investigate the thermo mechanical metallurgical interactions generated during cooling and heat treatment in order to find the origin of cracks. For this purpose, a thermo metallurgic mechanical finite element model is used. However these numerical simulations require a high amount of mechanical, thermal and metallurgical parameters. In order to determinate these parameters, a study of available data for estimation of mechanical parameters was performed. Thermo physical parameters were obtained by DTA and DSC methods. Metallurgical characterization by inverse numerical method based on available CCT diagrams was performed to determine the TTT diagrams. First cooling numerical simulations are presented, allowing a rough estimate of residual stresses values and the identification of key parameters for predicting accurate residual stresses by sensitivity analysis.

Key words: phase transformation, residual stresses, FE simulations, bimetallic rolls, cooling

1. INTRODUCTION

Bimetallic rolls are manufactured in Marichal Ketin industry (MK) using vertical spin casting process. As a first step, the shell material is poured into the mould in rotation, creating the shell of the roll. When solidification of this shell is almost reached, the core material is poured filling the mold. By this process, it is possible to obtain rolls with a high wear resistance due to the high alloyed chrome steel surface but also a high toughness and ductility in the cast iron core. Simulations are performed using a homemade finite elements code performing thermo mechanical metallurgical analysis (Habraken & Bourdouxhe, 1992). This model requires introducing mechanical, thermal and metallurgical parameters as input data. In this paper, several simulations have been performed in order to analyse the sensitivity of the results to the input data. In a first analysis, the influence of convective coefficient choice to predict the cooling rate is analysed as temperature has been measured only for some geometries. TTT diagrams are not available but recovered by inverse analysis on CCT of grades close from the ones used in the industry. As the reliability of these TTT diagrams is not perfect, a sensitivity analysis of results for dif-

ISSN 1641-8581

ferent TTT diagrams was performed. Finally modifications in mechanical input data are performed to analyse the effect of these parameters in the results, an analysis of data available in literature was performed to check the range of the material parameters used in the performed simulations. Currently the effect of transformation strain and plastic transformation strain are not yet studied but should be analysed in future. Thermo physical parameters are assumed as accurate as they were measured by experimental tests performed through DTA (differential thermal analysis) and DSC (differential scanning calorimetry) methods (Carton & Lecomte-Beckers 2009; Contrepois & Lecomte-Beckers, 2011).

This sensitivity analysis allows knowing the principal parameters that affect the prediction. This study guides the required effort in the determination of input data.

2. SELECTION OF INPUT DATA SET

2.1. Cooling rate

For rolls cooling simulations, in a first approach only the convective effects were simulated. It should be noted that radiation effects will be included in the following analysis. Industrial temperature measurements performed by MK allow the identification of the evolution of convective coefficient with temperature. This data set predicts a cooling curve at the surface of rolls taking around eight days to reach room temperature. However, a classical air cooling convective coefficient of constant value provides a different cooling rate taking only three days for the cooling. Corresponding cooling curves for both cases are shown in figure 1. This result demonstrates how sensitive is the cooling rate prediction to the convective coefficient.

2.2. TTT diagram

2.2.1. Core material

The core material is composed of a nodular graphite iron called hereafter SGI. The microstructure of the core material contains ferrite and pearlite in the matrix associated to uniformly distributed graphite nodules of various diameters. Matrix content was set to 70-80% Fe and 20-30%Pe by rough quantitative metallography assessment. The first TTT diagram considered in reference simulation was obtained by inverse numerical method (Neira, 2011) based on a set of experimental data founded in CCT diagram available (Röhrig & Fairhurst, 1979) and is shown in figure 2(a). Figure 2(b) shows TTT considered for the sensitivity analysis where the end curve of ferritic transformation is shifted in order to reach lower ferrite and higher pearlite.

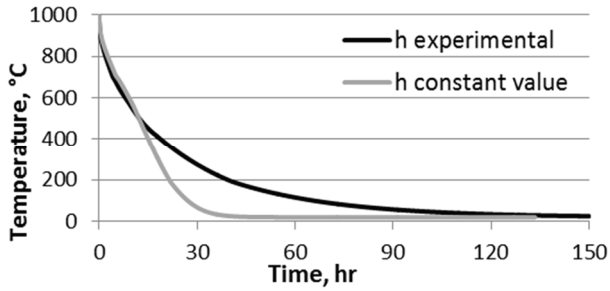

Fig. 1. Cooling curve for rolls surface.

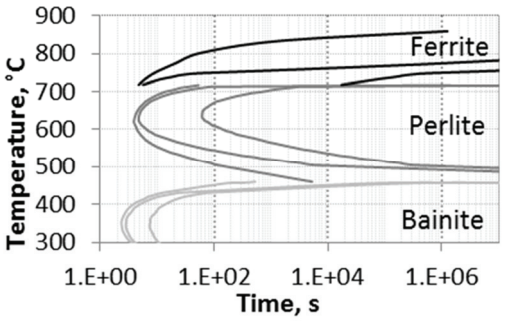

(a)

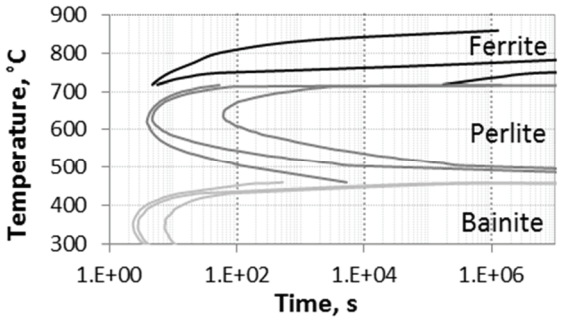

(b)

Fig. 2. TTT diagrams used for SGI (a) TTT diagram from inverse method (b) Modified TTT lower in ferrite.

2.2.2. Shell material

The shell material considered for manufactured rolls is a high chromium steel with a martensitic matrix with almost 10% of Cr carbides Cr_7C_3 and a small amount of Mo_2C, both located at the grain boundaries. Two cases were considered, in both cases TTT diagram shown in figure 3 obtained using also inverse numerical method to reach experimental data of computed CCT diagram (Neira, 2011) is used, however for the reference case only martensitic transformation is allowed. In the second case, in

order to analyse the sensitivity to the presence of a different phase in the matrix, bainitic and martensitic transformation have been allowed. This modification was performed because metallurgical analysis of this material, has detected troostite phase in martensitic matrix.

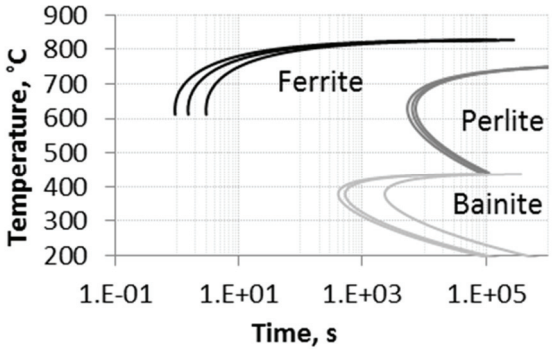

Fig. 3. *TTT diagram for HCS.*

2.3. Mechanical data

For determination of confident mechanical data, compression tests at constant strain will be performed. These tests will allow identification of Young modulus, Poisson modulus, plastic modulus and yield limit for each phase and for each material. Unfortunately, these tests are currently not performed. However it is possible to perform a study of available data in order to have an idea of future results and perform a sensitivity analysis.

For Young and Poisson modulus, curves for materials which belong to the same grade family were adopted. For Young modulus values from 42CD4 steel (Cassoto et al., 2005) for the shell, and C21980 (Herman, 2006) for the core were used. In the modified case for the sensitivity analysis we have introduced values of 60NCD11 (Denis et al., 1999) for

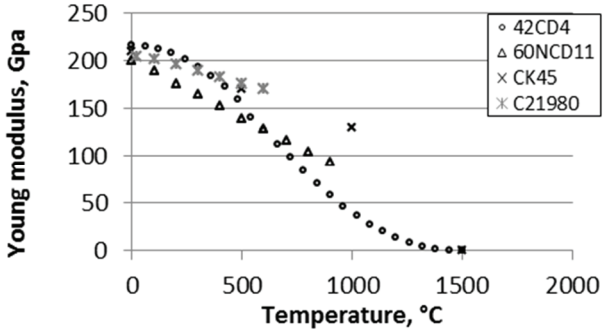

(a) Young modulus

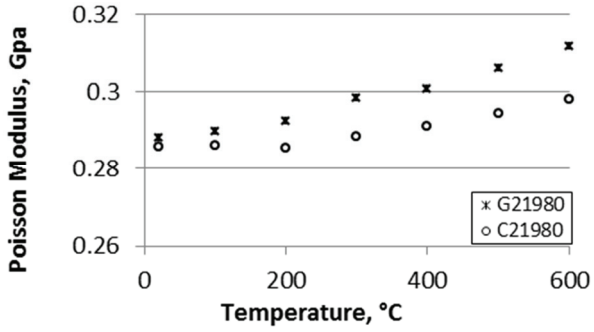

(b) Poisson modulus

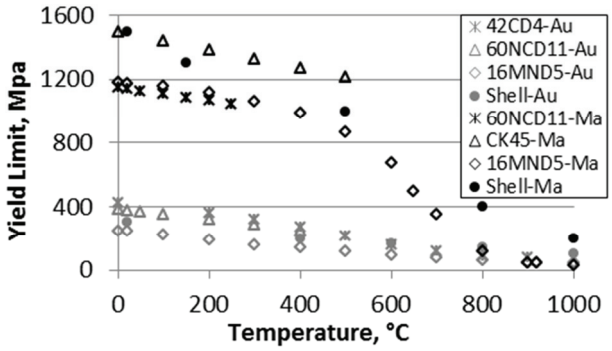

(c) Yield limit for austenite and martensite phases in the shell

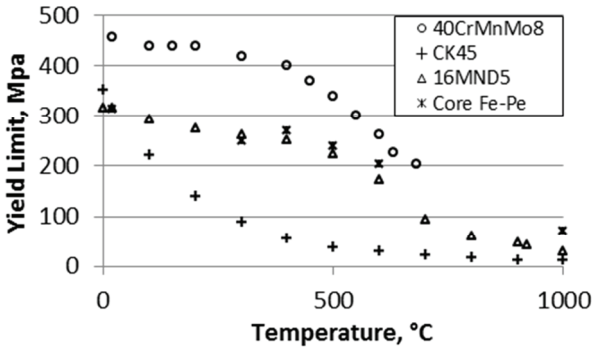

(d) Yield limit for ferrite and pearlite phases in the core

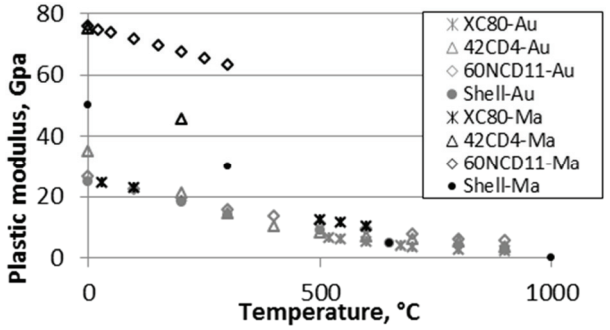

(e) Plastic modulus for austenite and martensite phases in the shell

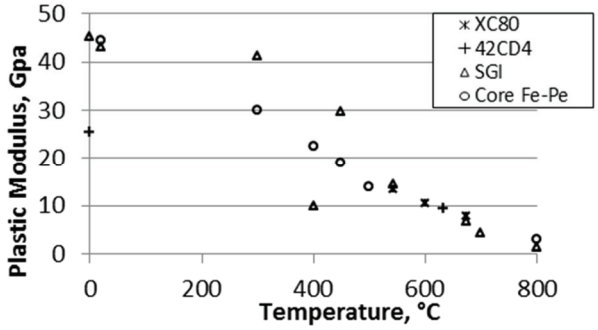

(f) Plastic modulus for ferrite and pearlite phases in the core

Fig. 4. *Chosen values of mechanical parameters for different phases compared to available data.*

shell and CK45 (Geijselaers, 2003) for the core. See figure 4(a) for the temperature dependence of the Young modulus. For Poisson modulus, due to the homogeneity of this parameter, no sensitivity is investigated, using G21980 (Herman, 2006) as shell data and C21980 (Herman, 2006) as core data, curves are shown in figure 4(b).

Table 1. *Summary of input data selection for different simulations.*

	Simulation	Convection h(T)	TTT diagram	σ - ε curve
1	Reference case	Experimental data from MK	Core: Obtained by inverse method Shell: Obtained by inverse method	Approach from available data and experimental points
2	Thermal modification	Constant value	Core: Obtained by inverse method Shell: Obtained by inverse method	Approach from available data and experimental points
3	Metallurgical modification	Experimental data from MK	Core: Slower ferritic transformation Shell: Allowing bainite transformation	Approach from available data and experimental points
4	Mechanical modification	Experimental data from MK	Core: Obtained by inverse method Shell: Obtained by inverse method	Data from similar materials

In the other hand, yield limit and plastic modulus, can present highly different values for different steels and phases. Available information for corresponding phases in similar materials was collected and some points corresponding to experimental data already available for core and shell materials (Studer, 2008; El Bartali et al., 2009), were used and extrapolated. It is possible to observe the chosen values for yield limit in figure 4(c) and (d), and for plastic modulus in figure 4 (e) and (f). For core material, yield limit and plastic modulus were considered as the same curve for ferrite and pearlite phases. As alternative data set for the sensitivity analysis, yield limit data of 60NCD11 steel (Denis et al., 1999) as shell, and 16MND5 (Coret, 2002) as core were used. For plastic modulus, alternative data used is the one of 60NCD11 steel (Denis et al., 1999) in shell and a close cast iron SGI (El Bartali et al., 2009) for the core.

2.4. Summary of input data

Table 1 summarizes the data choice for the different performed simulations. Assuming that simulation 1 is the most accurate one that current data allows, the simulations 2, 3 and 4 provide an idea of the effect of wrongs assumption on the results.

3. REFERENCE SIMULATION

3.1. Simulation geometry

Figure 5 explains the modelled geometry (El Bartali et al., 2009) and gives element numbers that allow understanding presented results. Element 1 is located in the centre of the cylinder, elements 40 and 41 define the interface between core and shell materials and element 77 reaches the surface layer. Free dilatation along Y axis is allowed but keeping parallel edges.

3.2. Results of the reference case

The results analysis helps to understand the phenomena happening in the roll during the cooling. Axial stresses and phase evolution as well as residual stresses will be extracted from the simulations. Figure 6 shows the evolution of axial stresses and phase transformation for different positions in the core. In red colour one can find the centre of the roll (element 1), in yellow and light blue core and shell side at interface are presented (elements 40 and 41 respectively), and finally in blue is shown the surface evolution (element 77). It is also possible to watch at the end of cooling, after 220hr the structure in the core is ferrite pearlite 82-18% volume and in the shell, the martensite volume reaches 50%, remaining material is austenite. Figure 7(a) presents axial stress and phase evolution in the first 80hr allowing observing the effect in the axial stress of phase transformation. Figure 7(b) shows the evolution of axial stresses with radius and time.

In figure 7(a) one can see that in the first 4hr of cooling, the stresses are increasing in both materials. The centre of cylinder is in compression, remainder material is in tension due only to thermal gradient.

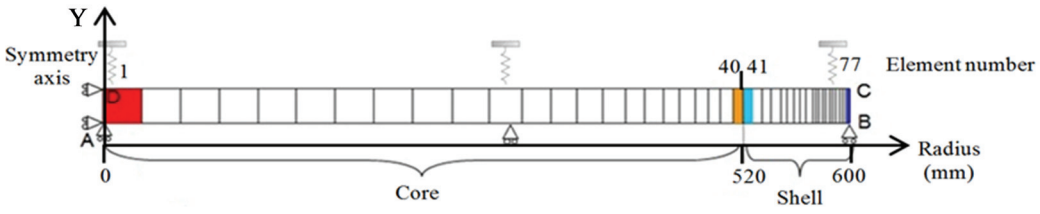

Fig. 5. *Geometry for axisymmetric simulation of the roll (El Bartali et al., 2009).*

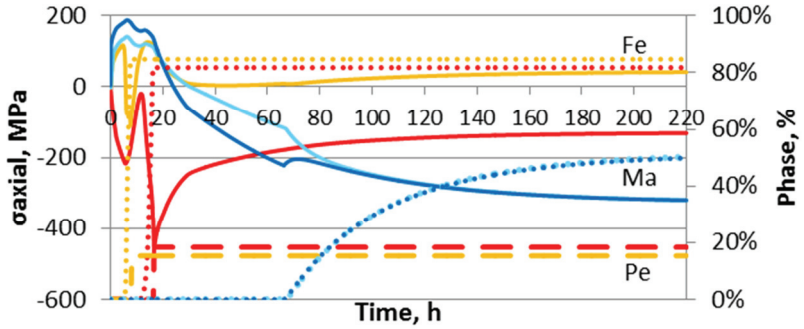

Core		
Element	1	40
σ axial		
% Fe		
%Pe		
Surface		
Element	41	77
σ axial		
% Ma		

Fig. 6. *Axial stress and phase evolution for core, surface of roll and interface between both materials.*

The first transformation in the roll is a ferritic one and starts in element 40, at t = 4.2 hr. This element is in compression due to the dilatation locally generated but restricted by the whole material, while the compression in element 1 will be reduced. At the same time, in the shell, tensile stress increases reaching 141 MPa and 187 MPa for element 41 and 77 respectively. Ferritic transformation goes on occurring element by element in the core generating high compressions balanced by tension in the shell and in the centre of the core until its own transformation. Before ferritic transformation occurs in element 1, pearlitic transformation also starts in element 40 at t = 7.67 hr. When element 1 is transformed, ferritic transformation starts at t = 10.4 hr and pearlitic transformation starts at t = 16.2 hr, a high compression is generated in this element reaching the maximal compression -473 MPa, due to the high stiffness in the core at this point. At t = 16.6 hr the whole core has been transformed into ferrite and pearlite. After that stage, stresses in the core are reduced and the shell goes from a high tension to a high compression. Martensitic transformation in the shell occurs almost at the same time for all the elements, starts in the element 77 at the surface at t = 66.3 hr and at t = 67.1 hr in element 41. This transformation generates dilatation which increases compression state in the shell and tension state in the core. At 220 hr the structure in the roll is 81.7%Fe-18.3%Pe in the core and 49.8%Ma at the surface. During cooling steps, it is also possible to compute the evolution of axial stresses with time in the whole cylinder; in figure 7(b) we can note that stresses are increasing with time. The shell and the centre of cylinder are in compression during the whole cooling, in the other hand the core is in tension for radius higher than 0.1 m. Blue curve gives results at the end of cooling. In the core, the residual stress is compression of -131 MPa for element 1 and 41.5 MPa for element

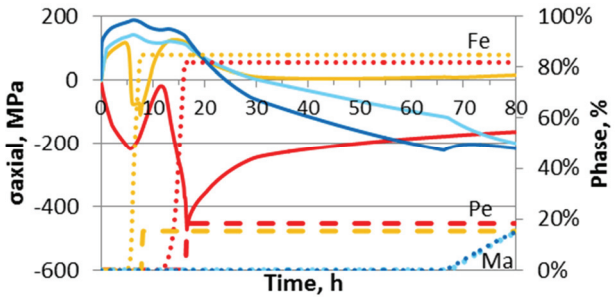

(a)

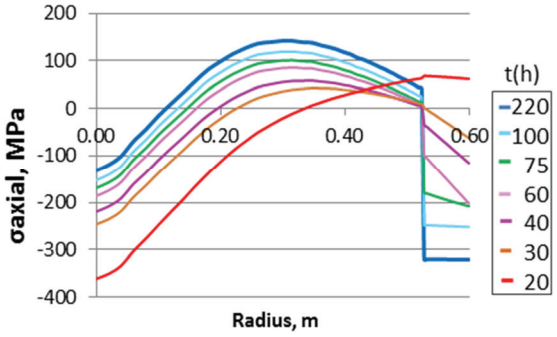

(b)

Fig. 7. *(a) Axial stress and phase rate evolution, zoom for first 80 hrs; (b) Axial stress along the radius for some cooling times.*

40. The maximal value for residual stress in the core corresponds to 142 MPa and this value is reached in the core at radius 0.298 m. In the shell, residual stress is compression equivalent to -320 MPa for element 41 and 77.

4. SENSITIVITY ANALYSIS

4.1. Thermal modification

Results obtained by simulations using a constant convective coefficient have shown that as it generates a higher cooling rate, martensite percentage at the surface increases slightly and reaches now 51.4%, see table 2. It generates at the same time, an increment in pearlite amount being more important in the external part of the core. As consequence, the axial stresses generated by phase transformations have globally increased. In addition, one can see in figure 8 that residual stresses have increased in the shell reaching -339 MPa and also in the core generating a maximal tension of 155 MPa at 0.298 m. However in the centre of the cylinder, it was decreased, obtaining -108 MPa.

Table 2. *Summary of results obtained for different simulations.*

Simulation		Phase percentage (%)			Maximal stresses (MPa)				
		Centre		Surface	At phase transformation		At the end of cooling		
		%Fe	%Pe	%Ma	σ core	σ shell	σ centre	σ max	σ surface
1	Reference case	81.7	18.3	49.8	-473	187	-131	142	-320
2	Thermal modification	81.4	18.6	51.4	-490	204	-108	155	-339
3	Metallurgical modification	67.0	33.0	42.8	-605	188	-311	131	-288
4	Mechanical modification	81.8	18.2	49.8	-447	254	-76.6	133	-321

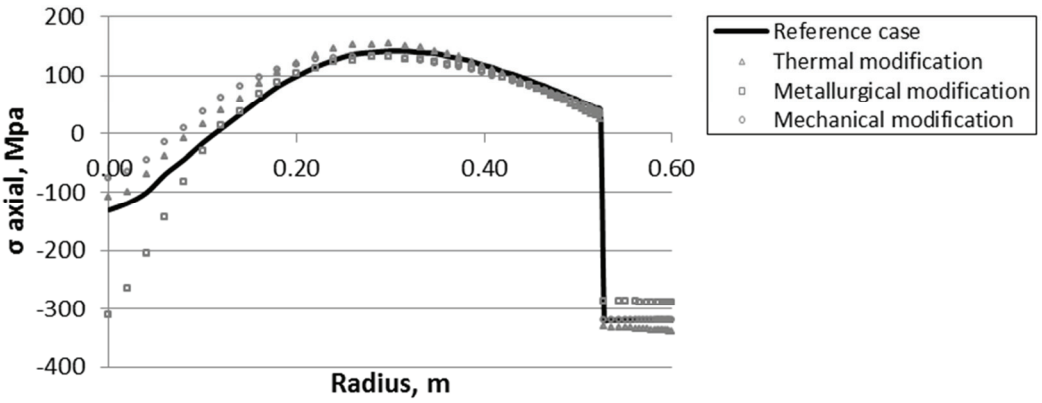

Fig. 8. *Residual stress comparison for different simulations.*

4.2. Metallurgical modification

It is possible to see that principal effects of modifications performed on TTT diagrams, are in the kinetic of phase transformations. In the core, the amount of pearlite phase is higher reaching 33% and in the shell, bainite phase is formed causing martensite percentage decrease until 42.8%, see table 2. As consequence, an increment in the stresses is generated in the centre either in values caused by phase transformation reaching compression of -605MPa or in residual stresses whose value achieves -311MPa. However the maximal residual tension in the core and residual stresses at the surface decrease until 131MPa and -288MPa respectively, see figure 8.

4.3. Mechanical modification

Introducing a different set of mechanical data produces no effect in phase rates. However, through these modifications, we can note in table 2 that axial stresses during phase transformation increases in the core reaching 254 MPa but decreases in the shell until -447 MPa. At the end of cooling, stresses decrease significantly in the core until -76.6 MPa in the centre and at 0.260 m where the maximal tension decreases until 133 MPa, moreover there is no effect in residual stresses for the shell, see table 2.

4.4. Summary of results

Results obtained by different simulations performed are summarized in table 2 allowing compari-

son of each modification performed with reference case. Values of stresses for the point of maximal tension in the core is included, corresponding to radius 0.298 m for simulation 1, 2, and 3, and to 0.260m for simulation 4. Residual stresses values are compared in figure 8 demonstrating the effect of each modification performed on residual stress.

5. DISCUSSION

Simulations performed allow understanding phenomena involved during cooling. For each modification performed on initial set of data, it has been possible to observe the effects on the predictions. For instance, if the martensite percentage obtained in the shell increases due to a higher cooling rate (simulation 2), then the residual stresses in the shell will increase but decrease in the core. Moreover if a lower martensite percentage is obtained (simulation 3), the residual stresses in the shell decrease but strongly increase in the core. This strong variation is also due to the increase of pearlite transformation. About stresses in the core due to transformations, occurring in the first hours of cooling, if pearlite phase volume increases as in simulations 2 and 3, maximal stresses increase. For mechanical modifications, as there is no effect in phase transformations, the effects are less significant. However the effect in the stresses is not negligible. It is important to note that residual compression stress in core centre is decreased and only for this case, the point of maximal tension generated in the core has been shifted.

6. CONCLUSION

- This model helps to clarify dependence of axial stresses with the amount of different phases.
- For a higher amount of pearlite in the core and martensite in the shell, increased values of axial stresses are generated.
- Simulation results are highly sensitive to metallurgical data. Modifications in TTT diagrams have generated the higher variations in the stresses, therefore it is important to consider the presence of troostite phase in the shell and the kinetic of ferrite and perlite transformation in the core.
- Modifications of mechanical data have also generated variations in values of stresses, however they are not as considerable as metallurgical effects.

Acknowledgments. The authors acknowledge Conicyt (National commission for scientific and technological research) Chile, for financial help. Interuniversity Attraction Poles Program-Belgian State - Belgian Science Policy P7 INTEMATE is thanked for its support. As research Director of FRS-FNRS, AM Habraken thanks this fund, for financial support.

REFERENCES

Carton, M., Lecomte-Beckers, J., 2009, *Rapport d'essais réalisés sur de matériaux de cœur*, Wallon region Project SOUBIRO, (in French).

Contrepois, Q., Lecomte-Beckers, J., 2011, *Analyses thermo physiques de l'acier haut chrome*, Wallon region Project SOUBIRO, (in French).

Casotto, S., Pascon, F., Habraken, A.M., Bruschi, S., 2005, Thermo-mechanical-metallurgical model to predict geometrical distortions of rings during cooling phase after ring rolling operations, *International Journal of Machine Tools & Manufacture*, 45, 657-664.

Coret, M., 2002, Experimental study of the phase transformation plasticity of 16MND5 steel low carbon steel under multiaxial loading, *International Journal of plasticity,* 18, 1707-1727.

Denis, S., Archambault, P., Aubry, C., Mey, A., Louin, J.C., Simon, A., 1999, Modeling of phase transformations kinetics and coupling with heat treatment residual stress predictions, *Journal de Physique IV, France*, 09, 323-332

El Bartali, A., Zhang, L., Studer, L., Habraken, A.M., 2009, Validation d'un calcul thermique métallurgique in Mécanique et mécanismes des changements de phases, *Proc. Conf. MECAMAT 2009*, eds, Appolaire, B., Arbab Chirani, S., Calloch, S., Denis, S., Leal, M., Tailleur, M., Aussois , France, 254-258, (in French).

Habraken, A.M., Bourdouxhe, M.,1992, Coupled thermo-mechanical-metallurgical analysis during the cooling of steel pieces, *European journal of mechanics - A/Solids*, 11, 381-402.

Herman, M., 2006, *Etude métallurgique et thermomécanique du phénomène de bris lors de traitements thermiques de cylindres de laminoir en acier moyen chrome*, PhD thesis, Université de Liège, (in French).

Geijselaers, H.J.M., 2003, *Numerical simulation of stresses due to solid state transformations: The simulations of laser hardening*, PhD thesis, University of Twente.

Neira, I., 2011, *Identificación de diagramas TTT a partir de diagramas CCT para modelación de transformaciones de fase,* Final work, Universidad de Concepción, (in Spanish).

Röhrig, K., Fairhurst, W., 1979, *ZTU-Schaubilder Giesserei,* Verlag, Düsseldorf, (in German).

Studer, L., 2008, *Modelling vertical spincasting of large bimetallic rolling mills*, DEA thesis, Université de Liège.

PRZEWIDYWANIE METODĄ ELEMENTÓW SKOŃCZONYCH POWSTAWANIA NAPRĘŻEŃ WŁASNYCH W BIMETALOWYCH WALCACH ROBOCZYCH PODCZAS CHŁODZENIA

Streszczenie

Bimetalowe walce używane w grupie wstępnej walcowni taśm na gorąco powinny charakteryzować się zarówno wysoką odpornością na zużycie powierzchni jak i zwiększoną wytrzymałością materiału podstawowego. Omawiany w artykule bimetalowy walec można otrzymać poprzez pionowe odlewanie, następnie chłodzenie i obróbkę cieplną. W tego typu walcu wady powstają na etapie chłodzenia w trakcie odlewania lub nieco później, podczas obróbek cieplnych. Należy zatem szczegółowo przeanalizować zależności cieplno mechaniczno metalurgiczne zachodzące podczas chłodzenia i obróbki cieplnej, tak, aby możliwe było zdiagnozowanie pochodzenia pęknięć. W tym celu wykonuje się obliczenia numeryczne z wykorzystaniem cieplno mechaniczno metalurgicznego modelu elementów skończonych. Prawidłowe przeprowadzenie takich symulacji wymaga znajomości licznych parametrów materiału: mechanicznych, cieplnych i metalurgicznych. W analizowanym w pracy walcu parametry mechaniczne wyznaczono na podstawie analizy danych dostępnych w literaturze. Parametry termo-fizyczne otrzymano przy użyciu metod DTA i DSC. Wykresy TTT wyznaczono na podstawie obliczeń odwrotnych w oparciu o dostępne wykresy CCT. W artykule przedstawiono wstępne numeryczne symulacje chłodzenia, które pozwalają na przybliżone oszacowanie wartości naprężeń oraz na identyfikację, przy użyciu analizy wrażliwości, kluczowych parametrów dla dokładnego przewidywania naprężeń własnych.

Received: September 25, 2012
Received in a revised form: October 29, 2012
Accepted: November 3, 2012